

Chromanol 293B Binding in KCNQ1 (Kv7.1) Channels Involves Electrostatic Interactions with a Potassium Ion in the Selectivity Filter

Christian Lerche, Iva Bruhova, Holger Lerche, Klaus Steinmeyer, Aguan D. Wei, Nathalie Strutz-Seeböhm, Florian Lang, Andreas E. Busch, Boris S. Zhorov, and Guiscard Seeböhm

Physiology I, University of Tuebingen, Tuebingen, Germany (C.L., K.S., N.S.-S., F.L., A.E.B., G.S.); Department of Biochemistry and Biomedical Sciences, McMaster University, Hamilton, Ontario, Canada (I.B., B.S.Z.); Department of Neurology, University of Ulm, Ulm, Germany (H.L.); and Department of Anatomy and Neurobiology, Washington University School of Medicine, St. Louis, Missouri (A.D.W.)

Received October 19, 2006; accepted March 6, 2007

ABSTRACT

The chromanol 293B (293B, *trans*-6-cyano-4-(*N*-ethylsulfonyl-*N*-methylamino)-3-hydroxy-2,2-dimethyl-chroman) is a lead compound of potential class III antiarrhythmics that inhibit cardiac I_{Ks} potassium channels. These channels are formed by the coassembly of KCNQ1 (Kv7.1, KvLQT1) and KCNE1 subunits. Although homomeric KCNQ1 channels are the principal molecular targets, entry of KCNE1 to the channel complex enhances the chromanol block. Because closely related neuronal KCNQ2 potassium channels are insensitive to the drug, we used KCNQ1/KCNQ2 chimeras to identify the binding site of the inhibitor. We localized the putative drug receptor to the H5 selectivity filter and the S6 transmembrane segment. Single residues affecting 293B inhibition were subsequently identified through systematic exchange of amino acids that were either

different in KCNQ1 and KCNQ2 or predicted by a docking model of 293B in the open and closed conformation of KCNQ1. Mutant channel proteins T312S, I337V, and F340Y displayed dramatically lowered sensitivity to chromanol block. The predicted drug binding receptor lies in the inner pore vestibule containing the lower part of the selectivity filter, and the S6 transmembrane domain also reported to be important for binding of benzodiazepines. We propose that the block of the ion permeation pathway involves hydrophobic interactions with the S6 transmembrane residues Ile337 and Phe340, and stabilization of chromanol 293B binding through electrostatic interactions of its oxygen atoms with the most internal potassium ion within the selectivity filter.

KCNQ1 (Kv7.1, KvLQT1) channels are characterized by fast activation and delayed inactivation, but the coassembly with the accessory β -subunit KCNE1 (also named IsK or MinK; Takumi et al., 1988) results in slowly activating, non-inactivating potassium currents (Barhanin et al., 1996; Sanguinetti et al., 1996; Tristani-Firouzi and Sanguinetti, 1998). These heteromeric channels constitute the cardiac I_{Ks} conductance, a component of the delayed rectifier repolarizing current I_K (Barhanin et al., 1996; Sanguinetti et al., 1996). Mutations in either gene can impair channel function and

cause Long QT syndrome (<http://www.fsm.it/cardmoc/>; Keating and Sanguinetti, 2001).

Most known class III antiarrhythmic drugs block I_{Ks} , the rapid component of the delayed rectifier I_K , which is encoded by the *HERG* gene, and thereby cause prolongation of the cardiac action potential (Sanguinetti, 1992; Roden, 1993; Singh et al., 1998). However, these medications possess a proarrhythmic potential and in turn may also increase the risk of life-threatening arrhythmias (Roden, 1993; Singh et al., 1998). I_{Kr} blockade is also an undesirable side effect of systemic therapy by diverse antihistaminic, antibiotic, psychoactive, and gastrointestinal prokinetic agents (<http://www.torsades.org/medical-pros/drug-lists/drug-lists.htm>). The molecular binding site in *HERG* was identified for a series of *HERG* blockers (Sanguinetti et al., 2005).

Alternatively, selective blockade of I_{Ks} (KCNQ1/KCNE1)

This work was supported by Aventis Pharma Deutschland GmbH and a grant from the National Sciences and Engineering Research Council of Canada (to B.S.Z.). Computations were performed, in part, using the SHARCNET Supercomputer Centre at McMaster University.

Article, publication date, and citation information can be found at <http://molpharm.aspetjournals.org>.
doi:10.1124/mol.106.031682.

ABBREVIATIONS: *HERG*, human *ether-a-go-go*-related gene; 293B, chromanol 293B (*trans*-6-cyano-4-(*N*-ethylsulfonyl-*N*-methylamino)-3-hydroxy-2,2-dimethyl-chroman); TEVC, two-electrode voltage-clamp technique.

has been suggested as a basis for more effective class III antiarrhythmic drugs (Sanguinetti and Jurkiewicz, 1991; Yang et al., 2000; Gerlach, 2003). I_{Ks} is enhanced during β -adrenergic sympathetic stimulation, a known trigger of some forms of arrhythmias (Roden, 1993). Accordingly, prolongation of action potential duration by the selective I_{Ks} blocker chromanol 293B (293B) is greater after isoproterenol treatment (Schreieck et al., 1997; Bosch et al., 1998). Thus, chromanol 293B is a leading compound of a novel class of I_{Ks} blockers that share structural similarity with K_{ATP} channel openers (Gerlach et al., 2001; Gerlach, 2003).

Determination of the binding sites of several K^+ channel blockers has increased our understanding of channel-drug interactions at the molecular level. Hanner et al. (2001), using binding studies, localized the correolide binding site in the central cavity of a three-dimensional Kv1.3 homology model. Mitcheson et al. (2000) determined the putative binding site of HERG-blockers in the central cavity by Alanine-scanning combined with functional inhibition of channels by blockers. Subsequent studies on Kv1.5 blockers and our own work on KCNQ1 also localized inhibitor binding sites to the central cavity (Seeböhm et al., 2003a; Decher et al., 2004), therefore suggesting that the central pore cavity of Kv-channels represents a preferential binding site for potent small-molecule inhibitors conserved in different potassium channel families. In all these studies, binding of the ligands to their receptors seems to depend mainly on hydrophobic and van der Waals interactions.

The recent definition of the binding sites of a blocking and a partially agonistic benzodiazepine (Seeböhm et al., 2003a,b) and the generation of a pharmacophore model (Du et al., 2005) enhanced our knowledge of the molecular mechanisms involved in KCNQ1 channel block. This pharmacophore model suggested the importance of three hydrophobic and one central aromatic interactions. The hydrophobic regions within the pharmacophore are supposed to be approximately 9.1, 11.5, and 12.6 Å apart from each other. These distances are in good agreement with the putative high-affinity binding mode of the benzodiazepine blocker L735821 (Seeböhm et al., 2003a) but do not satisfactorily explain the mode of binding of 293B, which is too small to fit the pharmacophoric points. The 293B molecule possesses a chroman scaffold to which an electron withdrawing cyano group is attached at the aromatic ring, which renders the molecule highly lipophilic, thereby favoring interactions with aromatic ring systems and hydrophobic side chains. Because 293B contains only a single hydrophobic area, it does not exactly match the pharmacophoric features of the model proposed by Du et al. (2005).

To gain insight into the molecular requirements of 293B action, we pursued a combined domain transplantation and site-directed mutagenesis approach to test candidate positions in the pore region for participation in drug binding. By this, we identified the H5/S6 domain as critical for drug sensitivity. Docking chromanol into closed and open conformations of KCNQ1 pore models based on the crystal structures of KcsA and Kv1.2 predicted binding of the ligand in the central cavity involving interactions with residues Ile337 and Phe340 and the most internal K^+ ion in the selectivity filter.

Materials and Methods

Molecular Biology. Molecular biological procedures were performed as described previously (Seeböhm et al., 2001b). For chimera construction, silent mutations were introduced that produced restriction endonuclease sites at corresponding positions in KCNQ1 and KCNQ2 flanking the region encoding the channel pore (SacI at amino acids "EL" 361/362, NsiI at amino acids "DAL" 301/302/303, and BamHI at amino acids "GS" 348/349 in KCNQ1). Other chimeric joining regions were created by recombinant PCR, resulting in constructs shown in Fig. 2. The megaprimer method was used for site-directed mutagenesis using cloned PfuI DNA polymerase (Promega GmbH, Mannheim, Germany). All constructs were verified by automated DNA sequencing. KCNQ cDNA constructs in pSGEM were linearized with NheI, and cRNA was synthesized by in vitro transcription (mMessage mMachine T7 kit; Ambion, Applied Biosystems, Darmstadt, Germany). CRNA concentrations were determined by photospectrometry, and transcript quality was checked by agarose gel electrophoresis. Enzymes were purchased from New England Biolabs (Ipswich, MA) if not otherwise stated. Sequences of cDNA clones were as given in GenBank: human KCNQ1, GenBank accession no. XM_052604.2; human KCNQ2, accession no. AF110020; rat KCNQ3, accession no. NM_032597; human KCNQ4, accession no. NM_004700; human KCNQ5, accession no. NM_019842; human KCNE1, accession no. NM_000219; KQT1, accession no. AY572974).

Two-Electrode Voltage-Clamp Technique. TEVC was performed as reported previously (Lerche et al., 2000a; Seeböhm et al., 2001a). In brief, *Xenopus laevis* ovaries were obtained from tricaine methanesulfonate-anesthetized animals. Oocytes were collagenase-treated (1 mg/ml, type IIL; Worthington Biochemicals, Freehold, NJ) in OR2 solution (82.5 mM NaCl, 2 mM KCl, 1 mM $MgCl_2$, and 5 mM HEPES, pH 7.4) for 120 min and subsequently stored in recording solution ND96 (96 mM NaCl, 2 mM KCl, 1.8 mM $CaCl_2$, 1 mM $MgCl_2$, and 5 mM HEPES, pH 7.4) with additional sodium pyruvate (275 mg/l), theophylline (90 mg/l), and gentamicin (50 mg/l) at 18°C. Each oocyte was injected with 10 ng of cRNA encoding either wild-type or mutant KCNQ subunits, or coinjected with either wild-type or mutant KCNQ1 (10 ng) and KCNE1 (5 ng). Standard TEVC recordings were performed at 22°C with a Turbo Tec 10CX amplifier (NPI Electronic GmbH, Tamm, Germany), an ITC-16 interface combined with Pulse software (HEKA, Lambrecht/Pfalz, Germany), and Origin version 6.0 (OriginLab Corp, Northampton, MA) for data acquisition. Macroscopic currents were recorded 3 to 4 days after injections. Pipettes were filled with 3 M KCl and had resistances of 0.5 to 1.5 MΩ. Proper voltage clamp was provided using the amplifier's integrator and visual control of the proportional-integral controller. Chromanol 293B was synthesized by the medicinal chemistry group of Sanofi-Aventis Pharma (Frankfurt, Germany). Chromanol 293B-containing solutions were freshly prepared from a 100 mM dimethyl sulfoxide stock solution. The maximal achievable 293B concentration was 100 μM. Chemicals were purchased from Sigma-Aldrich Chemie GmbH (Munich, Germany) if not stated otherwise. Student's *t* test was used to test for statistical significance, which was assumed at $p < 0.05$ (indicated by asterisk).

Molecular Modeling. Molecular modeling was performed using the ZMM program (<http://www.zmmsoft.com>), which employs the Monte Carlo minimization algorithm to search for optimal conformations (Li and Scheraga, 1987). Atom-atom interactions were calculated using the AMBER force field (Weiner et al., 1984). A cut-off distance of 8 Å was used. Hydration energy was calculated using the implicit-solvent method (Lazaridis and Karplus, 1999). Ionizable residues of the protein were kept in the neutral form (Momany et al., 1975; Lazaridis and Karplus, 1999).

The X-ray structures of KcsA (Doyle et al., 1998) and Kv1.2 (Long et al., 2005) served as templates for closed and open conformations of the KCNQ1 channel S5/H5/S6 domain, respectively. The alignment is shown in Table 4. The extracellular H5 loop residues in KCNQ1 (amino acids 291–294), which are not present in KcsA and Kv1.2,

were not modeled. These loops are too far from the ligand-binding site; therefore, this approximation does not affect our results. During energy minimizations, the α carbons of the proteins were constrained to corresponding positions of the templates using pins. The pins are flat-bottomed constraints, which allow penalty-free deviation up to 1 Å and impose a penalty of 10 kcal/mol/Å for deviations >1 Å. The binding sites of K^+ ions in the selectivity filter are numbered from 1 to 4 starting from the extracellular side (Zhou and MacKinnon, 2003). Positions 2 and 4 were loaded with K^+ ions and positions 1 and 3, with water molecules.

Atomic charges in (3*R*,4*S*)-chromanol 293B were calculated by the AM1 method using MOPAC (<http://www.mopac.com>). Bond angles of the ligand were allowed to vary in energy minimizations. The optimal positions and orientations of the ligand in the closed channel were initially searched by generating 20,000 random starting points with the mass center occurring within a cylinder of 16 Å in diameter and 13 Å in length. The axis of the cylinder coincided with the long axis of the pore. In the open channel, the corresponding cylinder was 20×18 Å. The area of the random search covered the entire pore region, including interfaces between domains. From each starting position, the energy was minimized in the absence of the solvent. The energy-minimized conformations within 100 kcal/mol from the apparent global minimum were further energy-minimized in water until the last 1000 energy minimizations did not improve the best minimum found.

Results

Closely Related KCNQ Potassium Channels Differ in Their Chromanol Sensitivity. Different KCNQ channels were expressed in *X. laevis* oocytes, and their sensitivity to chromanol 293B was determined using the TEVC technique. Homomeric KCNQ1 channels were inhibited with an IC_{50} value of 26.9 ± 0.8 μ M (Figs. 1–3, Tables 1–3). Because heteromeric KCNQ1/KCNE1 subunits were more sensitive to 293B ($IC_{50} = 6.9 \pm 0.5$ μ M; Figs. 1B and 3, Tables 1 and 3) than KCNQ1 channels alone, this drug may exert an I_{Ks} preference in vivo. KQT-1, the KCNQ1 homolog from *Caenorhabditis elegans* (Wei et al., 2005), was also highly sensitive to 293B ($IC_{50} = 16.2 \pm 1.3$ μ M; Fig. 1H). Homomeric KCNQ5 currents were only moderately inhibited by 293B (Fig. 1G), whereas homomeric KCNQ2, KCNQ3, KCNQ4, and heteromeric KCNQ2/KCNQ3 channels were only slightly blocked by 100 μ M 293B (Fig. 1, C–F; Table 1).

Identification of Regions in KCNQ1 Responsible for Chromanol 293B Sensitivity. To elucidate the structural determinants of 293B sensitivity we studied a series of func-

tional chimeras between chromanol-sensitive KCNQ1 and insensitive KCNQ2 channel subunits (Fig. 2). Several of these chimeras were described previously and kinetically characterized (Seebach et al., 2001b). Because C-terminal tails of KCNQ channels mediate subunit assembly (Schmitt et al., 2000; Maljevic et al., 2003; Schwake et al., 2003), they could be involved in drug inhibition mediated by disruption of the channel complex. However, a KCNQ1 protein with a KCNQ2 C terminus (Q1tailQ2) still expressed currents with similar sensitivity to block by 293B as wild-type KCNQ1 currents ($IC_{50} = 27.8 \pm 3.1$ μ M, $n = 4$; data not shown), demonstrating that this area is not important for drug inhibition. The inverse chimera (Q2tailQ1) did not yield functional channels (data not shown).

Because the pore region is preferentially targeted by several potassium channel blocking drugs (Mitcheson et al., 2000; Hanner et al., 2001; Seebach et al., 2003a; Sanguinetti et al., 2005), we exchanged the S5/H5/S6 region of KCNQ1 and KCNQ2, to create the Q1S5S6Q2 and Q2S5S6Q1 chimeras. Q1S5S6Q2 was almost insensitive to chromanol 293B (20% block by 100 μ M 293B; Fig. 2A, top right; Table 2). On the other hand, 293B sensitivity could be transferred to KCNQ2 along with the S5/H5/S6 domain of KCNQ1 (Q2S5S6Q1; IC_{50} value of 56 μ M; Fig. 2A, top right; Table 2). These results clearly identified the pore region as the critical determinant of 293B activity. To further narrow the sites of 293B binding, we then exchanged smaller parts of the S5/H5/S6 domain. Substitution of the S5-H5 linker in KCNQ1 by the corresponding sequence of KCNQ2 (Q1S5linkerQ2; Fig. 2A, lower left) did not affect 293B sensitivity, although this region shows only low sequence similarity. Likewise, a KCNQ1 chimera containing S5 of KCNQ2 exhibited only slightly reduced 293B sensitivity (Q1S5Q2; Fig. 2A, bottom left). In contrast, KCNQ1 channels with S5 through H5 of KCNQ2 were dramatically less sensitive to 293B (Q1S5H5Q2, 35% block by 100 μ M 293B; Fig. 2A, bottom right), as was the case with KCNQ1 containing the H5-S6 linker and S6 segment of KCNQ2 (Q1H5S6Q2, less than 10% block by 100 μ M 293B; Fig. 2A, bottom right). These results revealed that the H5 selectivity filter and S6 transmembrane segment are the principal determinants of 293B affinity in KCNQ1.

Point Mutations of the KCNQ1 Pore. Alignment of protein sequences spanning H5 and S6 regions of all KCNQ

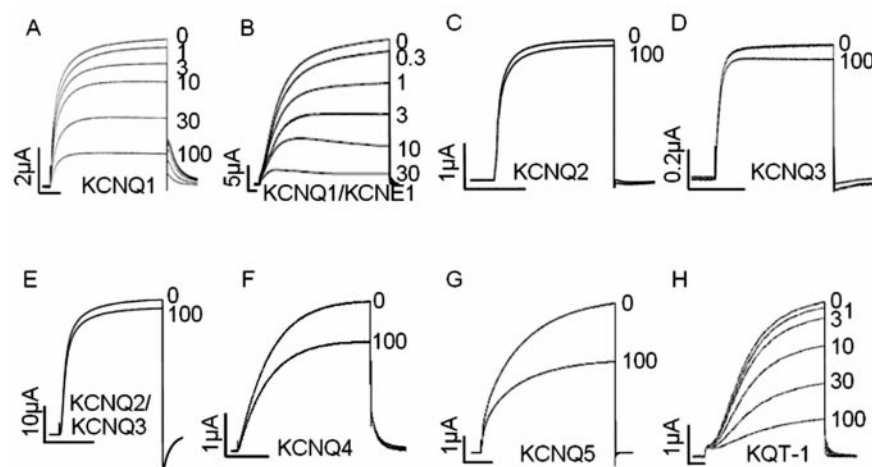


Fig. 1. Different 293B sensitivity of KCNQ channels. A–H, effect of 293B at indicated concentrations (in μ M) on different KCNQ channel currents elicited during voltage steps from -80 to $+40$ mV in oocytes ($n = 3$ –5). Horizontal scale bars represent 0.5 s.

channels identified several residues present in KCNQ1 as potential interaction partners of the 293B molecule (e.g., residues 307, 308, 326, 327, 330, 331, and 337, marked by arrows in Fig. 2B). We constructed KCNQ1 channels with either single or double substitutions of the corresponding amino acids of KCNQ2, and tested for inhibition by 293B (Table 3). Double exchanges at positions 326/327 and 330/331 did not significantly relieve the 293B block. However, single

point mutations V307L in the H5 pore helix and I337V in the S6 transmembrane helix significantly decreased the sensitivity to chromanol 293B (Fig. 3, A and C, Table 3).

Next, we introduced more conservative exchanges in the regions around residues Val307 and Ile337. We found that conservative mutation T312S strongly reduced current inhibition (Fig. 3G, Table 3), whereas the same mutation at the neighboring position, T311S, had no effect, and we found that

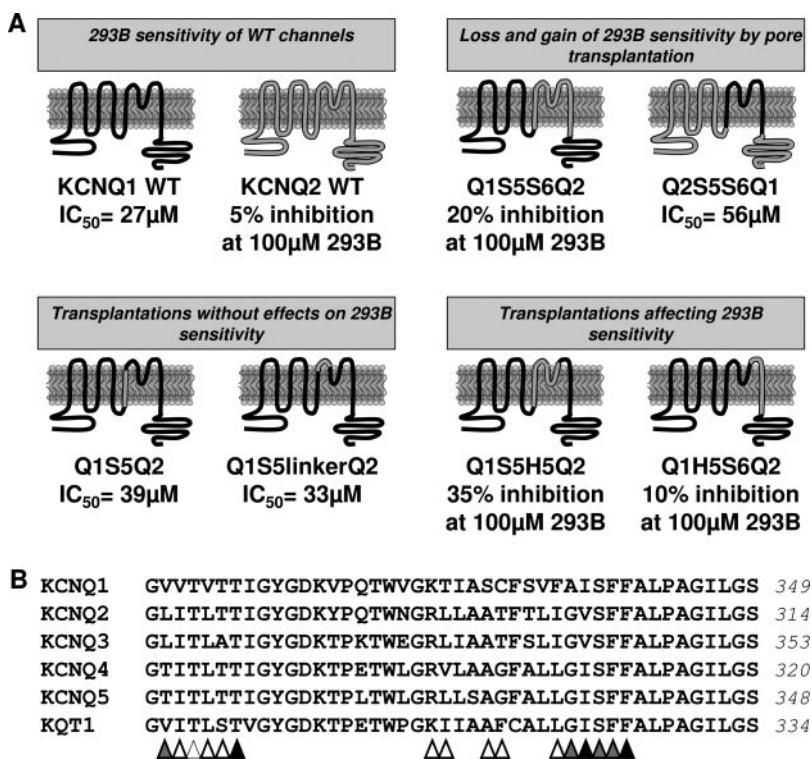


Fig. 2. Chimeras identifying important regions for chromanol 293B binding. A, models showing the typical backbone of a voltage-dependent potassium channel subunit with intracellular C and N termini and six transmembrane domains. Black and gray lines indicate KCNQ1 and KCNQ2 sequences, respectively. B, alignment of KCNQ channel protein sequences of H5 pore loop and S6 transmembrane regions. Differences in amino acids are marked by arrows. Positions of mutations with neutral effects on 293B affinity are marked by white arrows, and those with mild and strong effects with gray and black arrows, respectively.

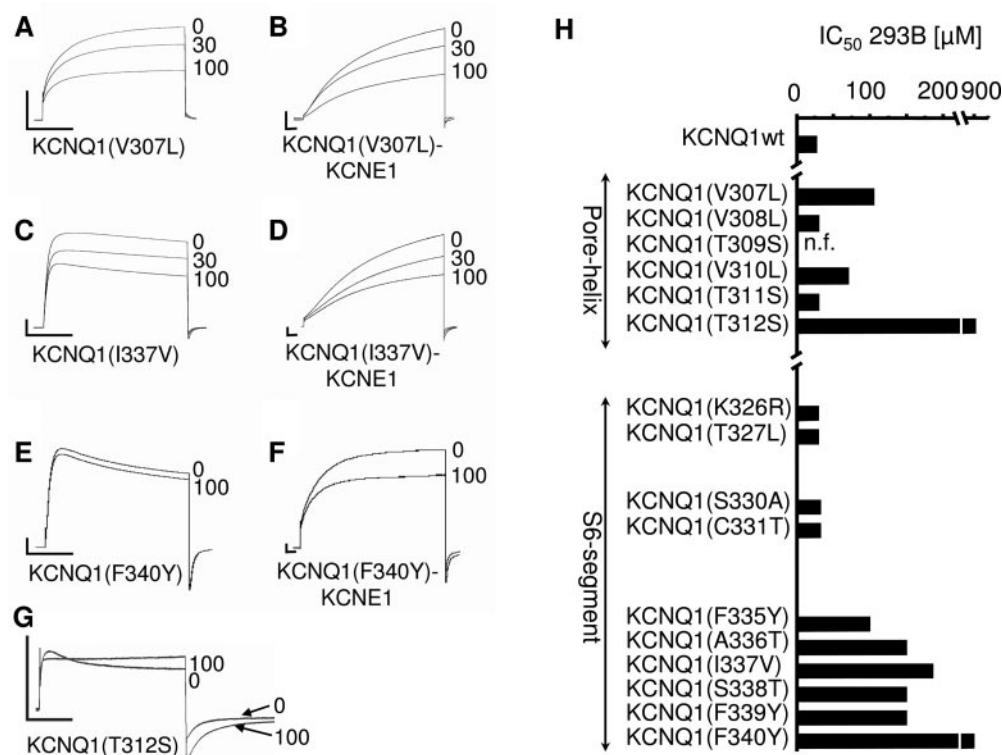


Fig. 3. Point mutations decrease chromanol sensitivity in KCNQ1. A–G, currents of indicated KCNQ1 mutants recorded in the absence or presence of KCNE1 before and after treatment with chromanol 293B. Currents were recorded in oocytes ($n = 3–8$) during voltage steps from -80 to 40 mV. KCNQ1 T312S/KCNE1 mutant currents could not be differentiated from endogenous *X. laevis* KCNQ1/KCNE1 currents when injected with KCNE1 only and are not shown. Horizontal scale bars represent 1 s; vertical scale bars represent 1 μA. H, bars represent mean IC₅₀ values of chromanol block ($n = 3–8$). The exact IC₅₀ values are summarized in Table 3. As a result of solubility, the maximum used concentration of chromanol 293B was 100 μM. IC₅₀ values above 100 μM were calculated assuming a Hill coefficient of 1.

mutation V310L caused a 2.6-fold decrease in sensitivity to 293B block (Table 3). Mutations around position Ile337 generally decreased sensitivity to 293B, and mutating Phe340, which is strictly conserved in all KCNQ channels, to tyrosine or isoleucine caused the strongest reduction in 293B sensitivity (Fig. 3, Table 3). In summary, the strongest effects on 293B block occurred by mutating a single residue (Thr312) in the lower selectivity filter and two residues in the central cavity, namely Ile337 and Phe340.

Introduction of Chromanol 293B Sensitivity into KCNQ2. To corroborate our findings, we introduced the identified amino acids into the KCNQ2 channel (Val307 and Ile337 in KCNQ1 correspond to Leu272 and Val302 in KCNQ2, respectively, Fig. 2B). In fact, these reciprocal sub-

stitutions (KCNQ2 L272V/V302I) increased 293B sensitivity 7-fold compared with wild-type KCNQ2 (34.7 ± 1.7 versus $5.0 \pm 1.0\%$ inhibition at $100 \mu\text{M}$, $n = 3$, Fig. 4). These experiments confirmed the importance of these two residues for the sensitivity of KCNQ1 channels to 293B block.

KCNE1 Effects on Channel Gating and 293B Block Can Be Functionally Separated. Because KCNE1, in addition to slowing activation kinetics and increasing current amplitudes, also increases 293B sensitivity of KCNQ1, we also investigated chromanol block of mutant KCNQ1 subunits in the presence of KCNE1. With mutants V307L, I337V, and F340Y, activation kinetics were slowed after co-expression with KCNE1, similar to that for wild-type KCNQ1. Mutant T312S, which generates only small currents, also did not show increased I_{Ks} -like currents; therefore, we could not test 293B sensitivity of these mutant heteromeric channels. However, coexpressed KCNE1, although it showed typical effects on current gating and amplitude, no longer augmented the sensitivity to 293B of KCNQ1 mutants V307L and I337V (Fig. 3, A–D; Table 3). These findings indicate that modulatory effects of KCNE1 on chromanol 293B pharmacology and on activation kinetics of resulting I_{Ks} currents can be functionally separated.

Molecular Modeling of the KCNQ1 Chromanol 293B Binding Site. To further corroborate the results from our functional expression studies, we performed extensive molecular modeling. We used the X-ray coordinates of KcsA and Kv1.2 crystal structures to construct homology models of the closed and open KCNQ1 pore, respectively (based on the protein sequence alignment shown in Table 4), and subsequently docked 293B into the pore models. Because our previous work on state-dependent binding of chromanol suggested a preferential open channel block mechanism (Seeböhm et al., 2001a), we first investigated the open pore conformation. Twenty thousand orientations of the ligand were randomly sampled in the Kv1.2-based model of the open KCNQ1 channel pore (Fig. 5, A and B). Several ligand-receptor complexes were found with the ligand-receptor energy within 5 kcal/mol from the apparent global minimum (Fig. 5, C and D). In these energetically most favored complexes, the largest stabilizing contribution to the binding of chromanol is

TABLE 1

293B sensitivity of KCNQ channels

IC₅₀ values are expressed as mean \pm S.E.M. n indicates number of experiments.

Channel	IC ₅₀	Inhibition at 100 μM 293B	n
	μM	%	
KCNQ1	26.9 ± 0.8		5
KCNQ1/KCNE1	6.9 ± 0.5		5
KCNQ2		~ 5	3
KCNQ3		~ 5	3
KCNQ4		~ 10	5
KCNQ5		~ 40	3
KQT1	16.2 ± 1.3		3
KCNQ2/KCNQ3		~ 5	3
KCNQ3/KCNQ5		~ 25	3

TABLE 2

293B sensitivity of wild-type and chimeric KCNQ1/KCNQ2 channels

IC₅₀ values are expressed as mean \pm S.E.M. n indicates number of experiments.

Channel	IC ₅₀	Inhibition at 100 μM 293B	n
	μM	%	
KCNQ1	26.9 ± 0.8		5
KCNQ2		~ 5	3
Q1S5S6Q2		~ 20	3
Q2S5S6Q1	56.2 ± 1.6		6
Q1S5Q2	38.7 ± 2.9		4
Q1S5linkerQ2	32.5 ± 2.1		3
Q1S5H5Q2		~ 35	3
Q1H5S6Q2		~ 10	3

TABLE 3

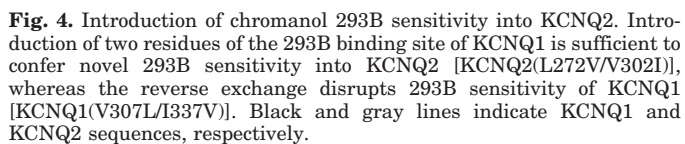
293B sensitivity of mutant KCNQ1 channels

IC₅₀ values are expressed as mean \pm S.E.M. n indicates number of experiments.

Mutation in KCNQ1	KCNQ1			KCNQ1/KCNE1 (I_{Ks})		
	IC ₅₀	Inhibition at 100 μM 293B	n	IC ₅₀	Inhibition at 100 μM 293B	n
	μM	%		μM	%	
KCNQ1 wild type	26.9 ± 0.8		5	6.9 ± 0.5		5
V307L		48.7 ± 3.2	4		49.9 ± 2.2	4
V310L	70.5 ± 2.1		3	30.5 ± 1.1		3
T311S	30.1 ± 1.7		3	7.2 ± 0.7		3
T311A	No functional expression			Not tested		
T312S		~ 10	4		Not tested	
K326R/T327L	29.5 ± 1.1		3		Not tested	
S330A/C331T	32.4 ± 2.0		3		Not tested	
F335Y		~ 50	3	9.1 ± 2.5		3
A336T		~ 40	3		~ 50	3
I337V		~ 35	4		~ 39	4
S338T		~ 40	4	10.2 ± 3.7		4
F339Y		~ 40	3	20.2 ± 1.7		3
F340I		~ 20	3	Not tested		
F340Y		~ 10	4		~ 30	4

We next explored the possibility of chromanol binding to

The present investigation was performed to further the knowledge about the binding mode and blocking mechanism of 293B. Using a chimera and single-point mutational approach we identify residues in the S6 transmembrane domain (Ile337, Phe340) and lower selectivity filter (Thr312) of the channel as crucial determinants of 293B sensitivity, strongly suggesting that the 293B receptor is located in the central pore cavity. To corroborate these experimental findings, we performed homology modeling and unbiased docking of chromanol in the closed and open KCNQ1 channels by generating a large number of starting conformations and energy-optimizing them. The obtained results confirm the mutagenesis data and propose that residues Ile337 and Phe340 essentially contribute to the ligand-receptor complex. It is noteworthy that nearby conservative exchanges F335Y, A336T, S338T, and F339Y also caused a significant reduction of 293B sensitivity. However, we believe that these ex-



The outer helices were aligned according to Bruhova and Zhorov (2005). 293B-sensing residues in the pore loop and inner helices of KCNQ1 are underlined.

Outer helix							
KcsA	14	KLLLGHRGSA	LHWRAAGAAT	VLLVIVLLAG	SYLAVLAERG	APGA	57
Kv1.2	313	GLQILGQTLK	ASMRELGLLI	FFLPFGVILF	SSAVYFAEAG	SENS	356
KCNQ1	247	TWRLGSGVVF	IHRQELITTL	YIGFLGLIFS	SYFVYLAEKD	AVNE	290
P-loop/H5							
KcsA	58	QLITYPRALW	WSVETATTVG	YGDLYPVT			85
Kv1.2	357	FFPSIPDAFW	WAVVSMTTVG	YGDMVPTT			384
KCNQ1	295	EFGSYADALW	WGVVTVTTIG	YGDKVPQT			422
Inner helix							
KcsA	86	LWGRLVAVVV	MVAGITSFGL	VTAALATWV	FV GREQ		120
Kv1.2	385	IGGKIVGSLC	AIAGVLTIAL	PVPVIVSNFN	YFYH		418
KCNQ1	423	WVGKTIASCF	SVFAISFFAL	PAGILGSGFA	LKVQ		456

changes rather alter the sterical configuration of the neighboring crucial residues Ile337 and Phe340, and/or hinder the access of 293B to the binding site. To corroborate this notion and the importance of the hydrophobic interactions with the cavity wall, we modeled the F340A mutant and then calculated the total energy of the ligand-receptor complex in this mutated channel. The obtained ligand-receptor energy of 293B was -17.8 kcal/mol, which indicates a significantly weaker binding as in the wild-type channel (-20.2 kcal/mol). Moreover, we found that the K^+ ion in position 4 of the selectivity filter is a further major contributor to the ligand-receptor binding energy. This suggests the formation of a tertiary complex between 293B, the permeating K^+ ion, and residues facing the cavity of the channel. Ligand-receptor interaction may be stabilized by the two oxygen atoms within

the sulfonamide (*N*-ethylsulfonyl-*N*-methylamino) group and the oxygen atom attached to C3 of the chroman ring, which together generate a negatively charged surface (Fig. 5I) and, according to our docking model, interact with the innermost potassium ion in the selectivity filter (K^+ at position 4). This prediction is further strengthened by the finding that substitution of the ethyl within the sulfonamide group by a bulkier substituent like butyl largely increases the IC_{50} value (Gerlach et al., 2001). A bulkier substituent presumably would weaken the interaction of the oxygens with the selectivity filter potassium ion. Substitutions at the aromatic ring with bulky lipophilic side chains (higher alkoxy substituents such as butoxy) increased the activity of the chroman structures to IC_{50} values as low as 50 nM (substance 8a in Gerlach et al., 2001), whereas substitution of the sulfonamide group

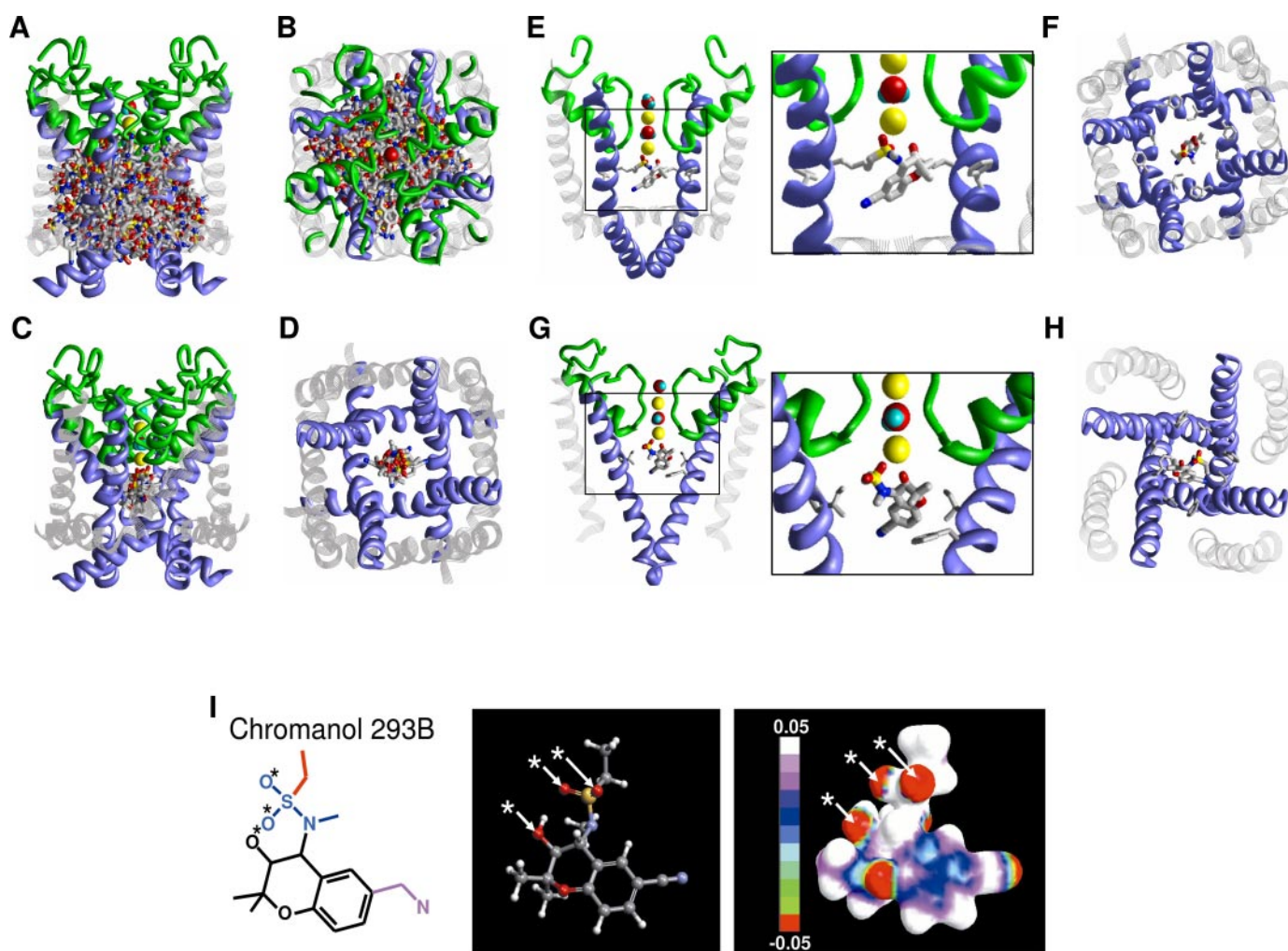


Fig. 5. Docking of a 293B molecule within the cavity of the homology models of the KCNQ1 channel. A–F, open channel model of KCNQ1 derived from the Kv1.2 X-ray structure. Side views (A and C), and top views (B and D) of random orientations of 293B inside the channel. A and B, only 200 of 20,000 positions are shown. C and D, superposition of the five most energetically favorable binding modes of 293B within the channel. E and F, typical low-energy binding mode of a 293B molecule within the cavity of the open channel. Residues Ile337 and Phe340 are shown as gray sticks. G and H, typical low-energy binding mode of a 293B molecule within the cavity of the closed channel derived from the KcsA X-ray structure. For clarity, hydrogen atoms are not shown. Only inner and outer helices of two subunits are shown in E and G. E and G contain close-up views. Potassium ions (in yellow) and water molecules (Corey-Pauling-Koltun code) are shown in space fill. The inner S5 helix is represented in purple; the pore helix, selectivity filter, and linkers are green; and the outer S6 helices are gray. I, structure of 293B molecule (*trans*-6-cyano-4-(*N*-ethylsulfonyl-*N*-methylamino)-3-hydroxy-2,2-dimethyl-chroman). Left, introduction of large substituents at the sulfonyl group (blue) at the site depicted in red were reported to increase IC_{50} values, whereas large hydrophobic substituents at C6 of the chroman (purple) decrease the IC_{50} . CPK-colored ball and stick model of 293B (middle). Right, 293B is depicted by surface-rendered representations. The coloring indicates the calculated electrostatic potentials \pm energy values (scale bar as indicated: $+0.05$ and -0.05 iso-valued surfaces). The two oxygen atoms of the sulfonyl group and the one attached to the chroman ring (at C3) represent a strong negative charge (red areas marked by * in the right-hand figure), which may be the molecular basis for a strong electrostatic interaction with the positively charged potassium ion in the lower selectivity filter.

with a pyrrolidine ring eliminated the block of the resulting substance (Gerlach et al., 2001). Both findings are consistent with our docking model. Finally, the sulfonyl group is attached to C4 and the oxygen atom, to C3 of the chroman ring. C3 and C4 represent chiral centers, and the 3*R*,4*S*-conformer shows a higher potency at opened channels in electrophysiological recordings. The position of the chroman ring relative to the three oxygen atoms depends on the chirality and thereby may determine the mode of drug interaction with Ile337, Phe340, and the potassium ion and 293B pharmacology (Yang et al., 2000; Seeböhm et al., 2001a). Other energetically less favored binding modes of the small 293B molecule in the channel cannot be fully excluded, but they would be less stable. The mode of drug interaction as proposed by the docking model implies that 293B inhibits KCNQ1 channel activity by a direct block of the ion permeation pathway.

The participation of conducting ions in the binding of ligands to the pore region was earlier proposed in molecular modeling studies of Ca²⁺ and Na⁺ channels (Zhorov and Ananthanarayanan, 1996; Zhorov et al., 2001; Tikhonov and Zhorov, 2005; Wang et al., 2006). Bruhova and Zhorov (2007) docked correolide inside the open homology pore of the Kv1.3 channel and found that the K⁺ ion in position 4 is an indispensable determinant of the correolide receptor. Correolide is much larger than chromanol 293B, but both drugs share common features that allow them to bind with high affinity to K⁺ channels. These include the ellipsoid-like shape with nucleophilic groups at the poles and hydrophobic sides. The drugs can reach the K⁺ ion bound to the cytoplasmic side of the selectivity filter by their polar groups, whereas their hydrophobic sides engage hydrophobic interactions with the predominantly hydrophobic inner helices.

How exactly does 293B block ion conduction? The hydrophobic and electrostatic interactions of 293B binding to the channel may ultimately disturb the coordination of the permeating potassium ions in the cavity and in the selectivity filter, which is of vital importance for ion conduction (Doyle et al., 1998; Roux and MacKinnon, 1999; Zhou and MacKinnon, 2004a,b). Mutations adversely affecting 293B block are consistently located near these sites in the cavity and base of the selectivity filter. In particular, the threonines at the base

of the selectivity filter (Thr312 in KCNQ1) are involved in the formation of K⁺-binding site 4. Furthermore, blocking activity of (3*R*,4*S*)-293B mildly increased with extracellular potassium (IC₅₀ at high extracellular K⁺, 10 ± 2 μM; IC₅₀ at low extracellular K⁺, 16 ± 4 μM; Seeböhm et al., 2001a). The X-ray structure of the KcsA channel showed that K⁺ ion concentration affects the equilibrium between distinct selectivity filter conformations (Zhou et al., 2001). At low K⁺ concentration (approximately 2 mM), the filter loses one of its dehydrated K⁺ ions and undergoes structural changes, whereas at higher K⁺ concentrations, the filter adopts a conductive conformation and occupancy of K⁺-binding site 4 may be increased (Zhou et al., 2001). This site coordinates the potassium ion predicted to interact with the 293B-oxygen atoms, and its increased occupancy thus in turn may stabilize (3*R*,4*S*)-293B-binding. Electrostatic interactions of permeating potassium ions with pharmacological reagents, as in case of the K_v channel blocker correolide (Bruhova and Zhorov, 2007), and as proposed here for 293B, may eventually be a frequent feature of K⁺ channel blocker interactions.

The modulatory role of the KCNE1 β-subunit in the sensitivity of the KCNQ1 channel to 293B is still not very well understood. The fact that KCNE1 increases the sensitivity to 293B but simultaneously relieves current inactivation already argues against stabilization of the inactivated state of the channel by 293B. Moreover, in the course of this work, we identified two KCNQ1 mutations, namely V307L and I337V, that eliminate the modulatory effect of KCNE1 on chromanol sensitivity but retain its effect on channel gating. One residue is located in the pore helix (Val307), and the other in the inner cavity (Ile337). Because KCNE1 possibly binds to the outer face of S6 and S5 (Tapper and George, 2000; Melman et al., 2004) and is not directly involved in formation of the central cavity and the selectivity filter, this could indicate that it does not directly take part in chromanol binding but acts allosterically to facilitate drug binding to the principal KCNQ1 subunit (Lerche et al., 2000b). Although our findings now suggest that facilitation of channel gating and 293B activity are independent actions of the accessory subunit, further studies are clearly necessary to elucidate the exact mechanisms of this modulatory interaction.

TABLE 5

Energy components (kcal/mol) of the most energetically favourable complexes of chromanol inside KCNQ1

Energy Component	Open Channel	Closed Channel
<i>kcal/mol</i>		
Ligand-receptor components		
van der Waals	-5.1	-13.8
Electrostatic	-26.7	-30.4
Solvation	12.2	14.8
Ligand components		
Intraligand nonbonded ^a	-9.6	0.6
Ligand strain ^b	9.0	16.2
Total	-20.2	-12.6
Major contributors to ligand binding energy ^c		
K ⁺ in position 4	-14.1	-13.3
H ₂ O in position 3	-1.4	-2.3
Thr311	-0.8	-4.9
Thr312	-1.9 (-2.2/1.9)	-1.8 (-4.7/4.6)
Ile337	-2.4	-3.6
Phe340	-0.8	-5.8

^a The sum of atom-atom interactions of the ligand.

^b The sum of energy of deformation of bond angles plus torsional energy of the ligand.

^c The energy contribution of a residue to ligand binding is summed over four subunits. The first number is the sum of contributions from the four domains. The values in parentheses show the minimal and the maximal contributions from individual domains.

Acknowledgments

We thank Michael C. Sanguinetti for fruitful discussion.

References

- Barhanin J, Lesage F, Guillemare E, Fink M, Lazdunski M, and Romey G (1996) Kv(L)QT1 and Isk (MinK) proteins associate to form the I(Ks) cardiac potassium current. *Nature (Lond)* **384**:78–80.
- Bosch RF, Gaspo R, Busch AE, Lang HJ, Li GR, and Nattel S (1998) Effects of the chromanol 293B, a selective blocker of the slow, component of the delayed rectifier K^+ current, on repolarization in human and guinea pig ventricular myocytes. *Cardiovasc Res* **38**:441–450.
- Bruhova I and Zhorov BS (2005) KvAP-based model of the pore region of Shaker potassium channel is consistent with cadmium- and ligand-binding experiments. *Biophys J* **89**:1020–1029.
- Bruhova I and Zhorov BS (2007) Monte Carlo-energy minimization of correolide in the Kv1.3 channel: Possible role of potassium ion in ligand-receptor interactions. *BMC Struct Biol* **7**:5.
- Decher N, Pirard B, Bundis F, Peukert S, Baringhaus KH, Busch AE, Steinmeyer K, and Sanguinetti MC (2004) Molecular basis for Kv1.5 channel block: conservation of drug binding sites among voltage-gated K^+ channels. *J Biol Chem* **279**:394–400.
- Doyle DA, Morais CJ, Pfuetzner RA, Kuo A, Gulbis JM, Cohen SL, Chait BT, and MacKinnon R (1998) The structure of the potassium channel: molecular basis of K^+ conduction and selectivity. *Science (Wash DC)* **280**:69–77.
- Du LP, Li MY, Tsai KC, You QD, and Xia L (2005) Characterization of binding site of closed-state KCNQ1 potassium channel by homology modeling, molecular docking, and pharmacophore identification. *Biochem Biophys Res Commun* **332**:677–687.
- Gerlach U (2003) Blockers of the slowly delayed rectifier potassium IKs channel: potential antiarrhythmic agents. *Curr Med Chem Cardiovasc Hematol Agents* **1**:243–252.
- Gerlach U, Brendel J, Lang HJ, Paulus EF, Weidmann K, Bruggemann A, Busch AE, Suessbrich H, Bleich M, and Greger R (2001) Synthesis and activity of novel and selective I(Ks)-channel blockers. *J Med Chem* **44**:3831–3837.
- Hanner M, Green B, Gao YD, Schmalhofer WA, Matyskiela M, Durand DJ, Felix JP, Linde AR, Bordallo C, Kaczorowski GJ, et al. (2001) Binding of correolide to the Kv1.3 potassium channel: characterization of the binding domain by site-directed mutagenesis. *Biochemistry* **40**:11687–11697.
- Keating MT and Sanguinetti MC (2001) Molecular and cellular mechanisms of cardiac arrhythmias. *Cell* **104**:569–580.
- Lazaridis T, and M. Karplus. (1999) Effective energy function for proteins in solution. *Proteins* **35**:133–152.
- Lerche C, Scherer CR, Seeböhm G, Derst C, Wei AD, Busch AE, and Steinmeyer K (2000a) Molecular cloning and functional expression of KCNQ5, a potassium channel subunit that may contribute to neuronal M-current diversity. *J Biol Chem* **275**:22395–22400.
- Lerche C, Seeböhm G, Wagner CI, Scherer CR, Dehmelt L, Aitbol I, Gerlach U, Brendel J, Attali B, and Busch AE (2000b) Molecular impact of MinK on the enantiospecific block of I(Ks) by chromanols. *Br J Pharmacol* **131**:1503–1506.
- Li Z and Scheraga HA (1987) Monte Carlo-minimization approach to the multiple-minima problem in protein folding. *Proc Natl Acad Sci USA* **84**:6611–6615.
- Long SB, Campbell EB, and MacKinnon R (2005) Crystal structure of a mammalian voltage-dependent shaker family K^+ channel. *Science (Wash DC)* **309**:897–903.
- Maljevic S, Lerche C, Seeböhm G, Alekov AK, Busch AE, and Lerche H (2003) C-terminal interaction of KCNQ2 and KCNQ3 K^+ channels. *J Physiol* **548**:353–360.
- Melman YF, Um SY, Krumer A, Kagan A, and McDonald TV (2004) KCNE1 binds to the KCNQ1 pore to regulate potassium channel activity. *Neuron* **42**:927–937.
- Mitcheson JS, Chen J, Lin M, Culbertson C, and Sanguinetti MC (2000) A structural basis for drug-induced long QT syndrome. *Proc Natl Acad Sci USA* **97**:12329–12333.
- Momany FA, McGuire RF, Burgess AW, and Scheraga HA (1975) Energy parameters in polypeptides. VII. Geometric parameters, partial atomic charges, nonbonded interactions, hydrogen bond interactions, and intrinsic torsional potentials of the naturally occurring amino acids. *J Phys Chem* **79**:2361–2381.
- Roden DM (1993) Torsade de pointes. *Clin Cardiol* **16**:683–686.
- Roux B and MacKinnon R (1999) The cavity and pore helices in the KcsA K^+ channel: electrostatic stabilization of monovalent cations. *Science (Wash DC)* **285**:100–102.
- Sanguinetti MC (1992) Modulation of potassium channels by antiarrhythmic and antihypertensive drugs. *Hypertension* **19**:228–236.
- Sanguinetti MC, Chen J, Fernandez D, Kamiya K, Mitcheson J, and Sanchez-Chapula JA (2005) Physicochemical basis for binding and voltage-dependent block of HERG channels by structurally diverse drugs. *Novartis Found Symp* **266**:159–166.
- Sanguinetti MC, Curran ME, Zou A, Shen J, Spector PS, Atkinson DL, and Keating MT (1996) Coassembly of Kv(L)QT1 and MinK (IsK) proteins to form cardiac I(Ks) potassium channel. *Nature (Lond)* **384**:80–83.
- Sanguinetti MC and Jurkiewicz NK (1991) Delayed rectifier outward K^+ current is composed of two currents in guinea pig atrial cells. *Am J Physiol* **260**:H393–H399.
- Schmitt N, Schwarz M, Peretz A, Aitbol I, Attali B, and Pongs O (2000) A recessive C-terminal Jervell and Lange-Nielsen mutation of the KCNQ1 channel impairs subunit assembly. *EMBO (Eur Mol Biol Organ) J* **19**:332–340.
- Schreieck J, Wang Y, Gjini V, Korth M, Zrenner B, Schomig A, and Schmitt C (1997) Differential effect of beta-adrenergic stimulation on the frequency-dependent electrophysiologic actions of the new class III antiarrhythmics dofetilide, ambasilide, and chromanol 293B. *J Cardiovasc Electrophysiol* **8**:1420–1430.
- Schwake M, Jentsch TJ, and Friedrich T (2003) A carboxy-terminal domain determines the subunit specificity of KCNQ K^+ channel assembly. *EMBO Rep* **4**:76–81.
- Seeböhm G, Chen J, Strutz N, Culbertson C, Lerche C, and Sanguinetti MC (2003a) Molecular determinants of KCNQ1 channel block by a benzodiazepine. *Mol Pharmacol* **64**:70–77.
- Seeböhm G, Lerche C, Pusch M, Steinmeyer K, Bruggemann A, and Busch AE (2001a) A kinetic study on the stereospecific inhibition of KCNQ1 and I(Ks) by the chromanol 293B. *Br J Pharmacol* **134**:1647–1654.
- Seeböhm G, Pusch M, Chen J, and Sanguinetti MC (2003b) Pharmacological activation of normal and arrhythmia-associated mutant KCNQ1 potassium channels. *Circ Res* **93**:941–947.
- Seeböhm G, Scherer CR, Busch AE, and Lerche C (2001b) Identification of specific pore residues mediating KCNQ1 inactivation. A novel mechanism for long QT syndrome. *J Biol Chem* **276**:13600–13605.
- Singh NA, Charlier C, Stauffer D, DuPont BR, Leach RJ, Melis R, Ronen GM, Bjerre I, Quattlebaum T, Murphy JV, et al. (1998) A novel potassium channel gene, KCNQ2, is mutated in an inherited epilepsy of newborns. *Nat Genet* **18**:25–29.
- Takumi T, Ohkubo H, and Nakanishi S (1988) Cloning of a membrane protein that induces a slow voltage-gated potassium current. *Science (Wash DC)* **242**:1042–1045.
- Tapper AR and George AL Jr (2000) MinK subdomains that mediate modulation of and association with KvLQT1. *J Gen Physiol* **116**:379–390.
- Tikhonov DB and Zhorov BS (2005) Sodium channel activators: model of binding inside the pore and a possible mechanism of action. *FEBS Lett* **579**:4207–4212.
- Tristani-Pirouzi M and Sanguinetti MC (1998) Voltage-dependent inactivation of the human K^+ channel KvLQT1 is eliminated by association with minimal K^+ channel (MinK) subunits. *J Physiol* **510** (Pt 1):37–45.
- Wang S-Y, Mitchell J, Tikhonov DB, Zhorov BS, and Wang GK (2006) How batrachotoxin modifies the sodium channel permeation pathway: computer modeling and site-directed mutagenesis. *Mol Pharmacol* **69**(3):788–795.
- Wei AD, Butler A, and Salkoff L (2005) KCNQ-like potassium channels in *Caenorhabditis elegans* conserved properties and modulation. *J Biol Chem* **280**:21337–21345.
- Weiner SJ, Kollmann PA, Case DA, Singh UC, Ghio C, Alagona G, Profeta S, and Weiner P (1984) A new force field for molecular mechanical simulation of nucleic acids and proteins. *J Am Chem Soc* **106**:765–784.
- Yang IC, Scherz MW, Bahinski A, Bennett PB, and Murray KT (2000) Stereoselective interactions of the enantiomers of chromanol 293B with human voltage-gated potassium channels. *J Pharmacol Exp Ther* **294**:955–962.
- Zhou M and MacKinnon R (2004a) A mutant KcsA K^+ channel with altered conduction properties and selectivity filter ion distribution. *J Mol Biol* **338**:839–846.
- Zhou Y and MacKinnon R (2003) The occupancy of ions in the K^+ selectivity filter: charge balance and coupling of ion binding to a protein conformational change underlie high conduction rates. *J Mol Biol* **333**:965–975.
- Zhou Y and MacKinnon R (2004b) Ion binding affinity in the cavity of the KcsA potassium channel. *Biochemistry* **43**:4978–4982.
- Zhou Y, Morais-Cabral JH, Kaufman A, and MacKinnon R (2001) Chemistry of ion coordination and hydration revealed by a K^+ channel-fab complex at 2.0 Å resolution. *Nature (Lond)* **414**:43–48.
- Zhorov BS and Ananthanarayanan VS (1996) Structural model of a synthetic Ca^{2+} channel with bound Ca^{2+} ions and dihydropyridine ligand. *Biophys J* **70**:22–37.
- Zhorov BS, Folkman EV, and Ananthanarayanan VS (2001) Homology model of dihydropyridine receptor: implications for L-type Ca^{2+} channel modulation by agonists and antagonists. *Arch Biochem Biophys* **393**:22–41.

Address correspondence to: Guiscard Seeböhm, Physiology I, University of Tuebingen, Gmelinstr. 5, D-72076 Tuebingen, Germany. E-mail: guiscard.seeböhm@gmx.de

Correction to “Chromanol 293B Binding in KCNQ1 (Kv7.1) Channels Involves Electrostatic Interactions with a Potassium Ion in the Selectivity Filter”

In the above article [Lerche C, Bruhova I, Lerche H, Steinmeyer K, Wei AD, Strutz-Seeböhm N, Lang F, Busch AE, Zhorov BS, and Seeböhm G (2007) *Mol Pharmacol* 71:1503–1511], the authors' corrections to the page proofs were not implemented as a result of a copyediting error. In addition, as the missing corrections were being prepared, a number of other items needing correction were noted. All of the corrections are detailed below.

Page 1503

In the affiliation line, a period was inserted after the first “S” in “N.S.-S.”, “and” was inserted before the last affiliation, “Saint Louis” was changed to “St. Louis”, and the period at the end of the line was deleted.

In the abbreviations list, line 2, a hyphen was inserted between “voltage” and “clamp” in the definition of TEVC.

Page 1504

In the first full paragraph of the left column, line 5, “Kv1.3” was inserted between “three-dimensional” and “homology.”

In the second heading under *Materials and Methods*, a hyphen was inserted between “Voltage” and “Clamp”.

In lines 14 and 15 of that section, a space was inserted after “amplifier” and before “(NPI...)”.

Page 1505

In the first paragraph of the right column, line 11, “ μM ” was inserted after “3.1” and before the comma.

In the next paragraph, lines 16 and 22, a comma was inserted after “Fig. 2A”.

Page 1506

In Fig. 3H, the asterisk following “KCNQ1(T312S)” and its bar was deleted. In the legend to Fig. 3, line 4, “the” was inserted between “in” and “absence”.

Page 1507

In the first heading in the left column, “sensitivity” was changed to “Sensitivity”.

In the section *KCNE1 Effects on Channel Gating and 293B Block Can Be Functionally Separated*, in the right column, line 6, “the” was inserted between “in” and “presence”. In line 10, “ I_{K_A} ” was changed to “ I_{K_A} ”.

In the legend to Table 3, the comma after “S.E.M.” was deleted. In the table itself, the following changes were made:

in the first line after the boxhead, “ μM ” was inserted under “ IC_{50} ” and “%” was inserted under “Inhibition at 100 μM 293B”. In line 2, column 2, the “ μM ” after “ 26.9 ± 0.8 ” was deleted. In line 3, column 6, the “%” after “ 49.9 ± 2.2 ” was deleted. In line 6, column 3, the “%” after “ ~ 10 ” was deleted. In line 11, column 6, “ ~ 394 ” was changed to “ ~ 39 ”.

Page 1508

In the right column, line 10, the word “bulky” was deleted.

In Fig. 4, an “L” was inserted before the solidus (/) in “KCNQ1(V307/I337V)”. In the legend to Fig. 4, lines 3 and 4, the hyphens in “293B-sensitivity” were deleted. In line 5, the parentheses around “KCNQ1(V307L/I337V)” were changed to square brackets.

In Table 4, a period was inserted at the end of the legend, and the stray period in the footnote was deleted.

Page 1509

In the right column, line 10, an “s” was added to “oxygen”.

In the legend to Fig. 5, line 1, the hyphen between “A” and “F” was changed to an N-dash (i.e., from - to –). In line 6, “2” was changed to “two”. In line 13, a hyphen was inserted between “right” and “hand”.

Page 1510

In the right column, line 10 from the bottom, “Jr” was deleted after “George” in the reference citation.

In Table 5, in the boxhead, “component” was changed to “Component”. In footnote a, a period was added to the end of the sentence.

Page 1511

In the reference list, the Zhou references were put in the correct order per journal style: Zhou M and Mackinnon, 2004a; Zhou Y and Mackinnon, 2003; Zhou Y and Mackinnon, 2004b; and Zhou Y, Morais-Cabral JH, et al.

The online version of this article has been corrected in departure from the print version.

The printer regrets these errors and apologizes for any confusion or inconvenience they may have caused.